JOURNAL OF OPTOELECTRONICS AND ADVANCED MATERIALS Vol. 10, No. 10, October 2008, p. 2727 - 2731

Hybrid precursors synthesis and photoluminescence of rare earth ions - activated $Sr_3Y(PO_4)_3$ phosphors

SHUAI XU, XIUZHEN XIAO, BING YAN*
Department of Chemistry, Tongji University, Shanghai 200092, China

Using rare earth coordination polymers with salicylic acid as precursors and composing with the polyvinyl alcohol (PVA) as dispersing media, Eu^{3+}, Tb^{3+}, Ce^{3+} – activated $Sr_3Y(PO_4)_3$ phosphors with different doping concentration and $Sr_3Y(PO_4)_3$: 3 mol % Pr^{3+} were prepared via an modified wet chemical technology. The emission intensities of activators have been found to depend strongly on the doping concentration. The result is that the optimum concentration for Eu^{3+} is 7 mol %, for Tb^{3+} is 9 mol % and for Ce^{3+} is 3 mol %, respectively. Furthermore, the crystal field depression value D (Ln, A) of $Sr_3Y(PO_4)_3$ have been calculated to be 16, 895 cm^{-1} when Ce^{3+} was doped in $Sr_3Y(PO_4)_3$.

(Received September 7, 2007; accepted August 14, 2008)

Keywords: Optical materials, Chemical synthesis, Luminescence, Optical properties, $Sr_3Y(PO_4)_3$ phosphors

1. Introduction

New materials crystallizing with eulytite (also called eulytine or agricolite) structure are gaining considerable attention these years because of their high performance. The structural type of eulytite was first recognized in mineral $Bi_4(SiO_4)_3$ (BSO), which belong to cubic space group, with Bi in the 16c, Si in the 12a and O in the 48e equipoints of space group $I\bar{4}3d$ [1]. A large number of compounds isostructural with this mineral have been reported over the past 20 years, such as $Bi_4(GeO_4)_3$, $Pb_3Bi(XO_4)_3$ (X = P, As, V), $Pb_3M(GeO_4)_3$ (M = M^{2+}), $M_3Ln(PO_4)_3$ (M = Ca, Sr, Ba, Pb; Ln = Lanthanide), $Pb_3M(PO_4)_3$ (M = V, Cr, Fe) and $Pb_{3.5}M_{0.5}(PO_4)_3$ (M = Ti, Th) [2-7]. Rare earth ions are well-known luminescent activators in a variety of host lattices and the rare-earth activated phosphors have been studied extensively because of their high light output, excellent color rendering index, energy efficiency and greater radiation stability [8 - 11]. In the same way, eulytite structuctral phosphates have been shown to be better hosts for rare earth ions [12 - 16]. $M_3La(PO_4)_3$: Ce^{3+} (M = Sr, Ba) phosphor has been reported by Hoogendorp et al [17] and Ce^{3+}, Pr^{3+},Tb^{3+} activated $Sr_3Ln(PO_4)_3$ luminescent materials have been fabricated by Liang et al and their photoluminescent spectra under VUV – UV excitation have been discussed in details [18]. But in most cases, they synthesized luminescent materials doped with rare earth ions have been prepared through solid-state reactions at temperatures above 1300 °C or other traditional ways [19 - 20]. Recently, it has been reported that a very useful synthesis technology which is based on hydrolysis and polycondensation process has been popular and has been put in synthesis of nonagglomerated nanoparticles [21 - 22].

At present, we have put forward a novel and modified in – situ wet chemical method to fabricate the luminescent materials. Rare earth coordination polymers with ortho-hydroxylbenzoic acids was used as rare earth species and composed with organic polymers as the hybrid precursors, which can be used to produce slighter agglomerated and well - dispersing materials [23 -26]. This pathway exhibits different advantages, mainly the implementation of rather soft temperatures to produce the materials. Accordingly, a control on the structure, morphology of particles, dispersion of the different metals, etc, is also possible. In this paper, we have synthesized $Sr_3Y(PO_4)_3$: RE^{3+} (RE=Eu, Tb, Pr, Ce) crystalline phosphors with different doping concentration and discussed the luminescent properties of rare earth ions in details.

2. Experimental

2.1 Synthesis of $Sr_3Y(PO_4)_3$: Eu^{3+}

The initiative material Y_2O_3 was firstly dissolved into concentrated nitric acids. Then Superfluous salicylic acid (6.0 mmol) was dissolved into 95 % ethanol and its pH value was then adjusted to 7.0 ~ 8.0 with ammonia solution. Then the $Y(NO_3)_3$ was added and mixed homogenously. After being stirred for half hours, the urea and PEG were added into the above solutions with appropriate ratio to RE. After an hour, the solutions were heated to 70 °C and the pH value was adjusted to 7.0 ~ 8.0. At the same time, the $NH_4H_2PO_4$ and $SrCO_3$ powders were

added into the solutions. After this, the solutions were stirred until they became homogenous systems. After being deposited for several days they were filtered and the precursors were achieved. Finally the samples were heat-treated at the temperature 1000℃ for about 2 hours.

The same synthesis process was employed in other rare earth ions – doped $Sr_3Y(PO_4)_3$ phosphors except for the different activator.

Physical measurements

The particle sizes were characterized by means of X-ray diffraction (XRD, Bruke, D8-Advance, 40 kV and 20 mA, CuKα). The morphology and micro structure were characterized with scanning electronic microscope (SEM, Philps XL-30). Excitation and emission spectra at room temperature were determined with Perkin-Elmer LS-55 model fluorophotometer (excitation slit width = 10 nm, emission width = 5 nm).

3. Results and discussion

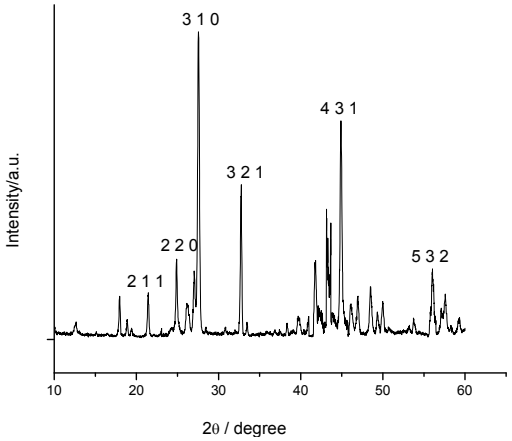

Fig. 1 The XRD patterns of the $Sr_3Y(PO_4)_3$: Ce^{3+} crystalline powders.

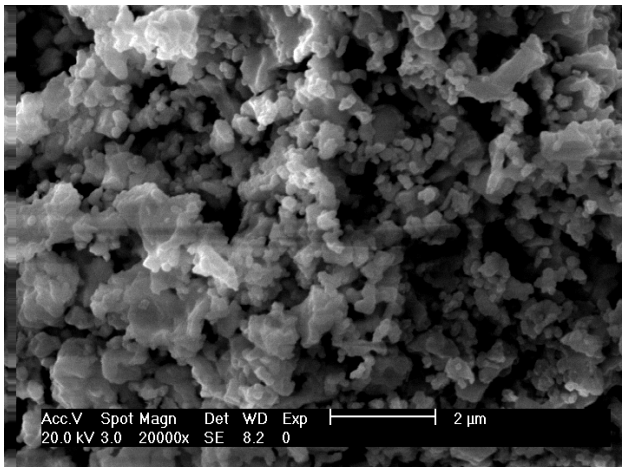

Fig. 2 SEM micron morphologies of $Sr_3Y(PO_4)_3$: Ce^{3+}.

Fig. 1 shows the XRD pattern of prepared samples checked by X – ray powder diffraction using Cu*Ka* radiation. The XRD data indicated that $Sr_3Y(PO_4)_3$ was single cubic phases and belong to the large family of the eulytite type compounds, which was in good agreement with those in JCPDS cards 44 – 0320. Using the scanning electron microscope (SEM) we obtain the morphology and the representative one of $Sr_3Y(PO_4)_3$: Eu^{3+} was shown in Fig. 2. As shown in Fig. 2, phosphor particle size is about 0.5 micrometer which takes agreement with the data from the XRD estimation (Fig.1). It can be seen that both of them mainly consist of solid micron crystalline structures. In addition, there exist some conglomeration phenomena in the SEM micrograph due to the higher temperature of thermal decomposition. It needs to refer that the crystalline particles and submicrometer to micrometer dimension for solid phosphors can be expected to achieve high strength and would be very useful for the application to obtain high efficiency. The products with micrometer crystalline particle result from the selection of Rare earth complexes with aromatic carboxylic acid (ortho hydroxylbenzoic acid) showing the polymeric structure as the rare earth species [27]. The organic polymer, polyethylene glycol (PEG) was combined both as dispersing medium and fuel to form the polymeric hybrid precursor template and show higher temperature of thermolysis process. These rare earth coordination polymers can compose with organic polymers (PEG) to obtain an interpenetrating polymeric network structures for they show the similar infinite polymeric structure [28]. After the decomposition of the hybrid precursors, $Sr_3Y(PO_4)_3$: Eu^{3+}, Tb^{3+}, Ce^{3+}, Pr^{3+} phosphors have been fabricated .

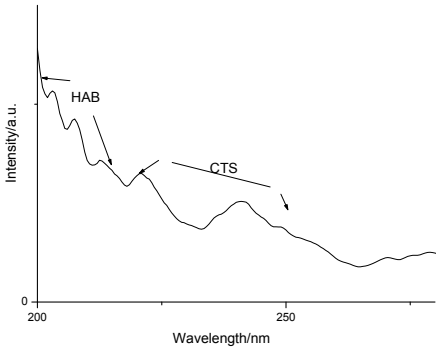

a

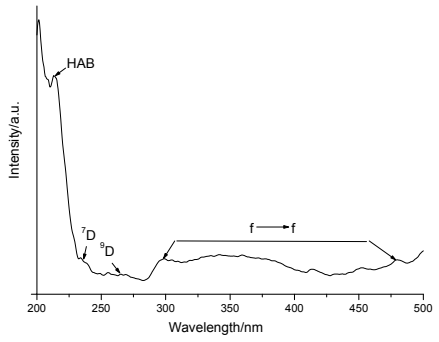

b

Fig. 3. Excitation spectra of $Sr_3Y(PO_4)_3$: Eu^{3+} a and $Sr_3Y(PO_4)_3$: Tb^{3+} b.

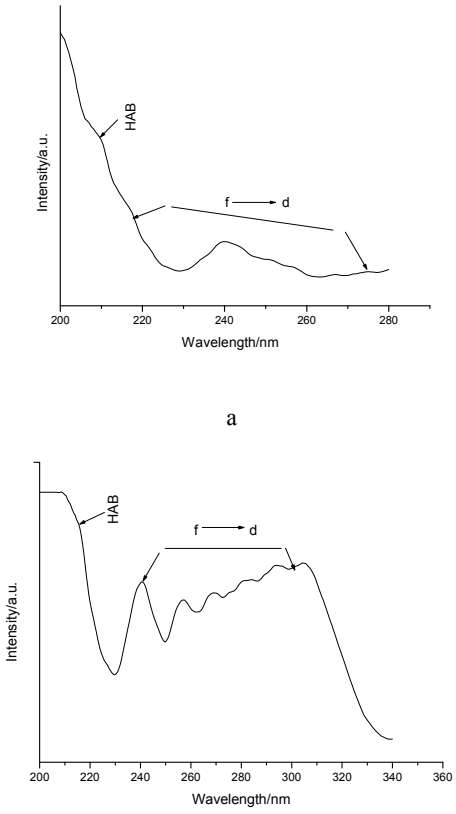

Fig. 4 Excitation spectra of $Sr_3Y(PO_4)_3$: Pr^{3+} (A) and $Sr_3Y(PO_4)_3$: Ce^{3+} (B).

All the excitation spectra of $Sr_3Y(PO_4)_3$: Eu^{3+}, Tb^{3+}, Ce^{3+}, Pr^{3+} show the similar features and the representative excitation spectra for $Sr_3Y(PO_4)_3$: $0.05Eu^{3+}$ and $Sr_3Y(PO_4)_3$: 0.05 Tb^{3+} annealed at 1000 °C are shown in Figs. 3 (A) and (B), respectively. Besides, For $Sr_3Y(PO_4)_3$: $0.05Pr^{3+}$ and $Sr_3Y(PO_4)_3$: $0.05Ce^{3+}$, the excitation spectra was given in Fig. 4 (A) and (B), respectively, which is monitored at an emission wavelength of 612 nm ($^3P_0$ to $^3H_6$ red emission) for Pr^{3+} system and of 386 nm ($^5D_2$ – $^7F_{7/2}$) for Ce^{3+} one. As for Eu^{3+}, several bands are observed in the range of 200 to 280 nm, such as host band around 210 nm and charge transfer band from O^{2-} to Eu^{3+} at 220 nm (Fig. 3 (A)). For Fig. 3 (B), the excitation spectra of $Sr_3Y(PO_4)_3$: Tb^{3+} activated powders presents three strong bands centered at 210, 243, 256 nm and a week band in the region 300 – 400 nm. The band at 210 nm was ascribed to the host absorption. The band at 220 nm would seem to be attributed to the ^7D level of the 4f – 5d transition of Tb^{3+} due to s spin-allowed $_4f^8$–$_4f^7{}_5d^1$ transitions, with higher energy and the band at 243 nm could be assigned to the ^9D level of the $_4f^7{}_5d^1$ configuration, with lower energy. Besides this, there also appeared a week band in the region 300 – 400 nm resulting from the Tb^{3+} f – f transition. For Fig. 4 (A), the bands around 210 nm are attributed to the host bands and these bands in the range of 220 to 280 nm, corresponding to the f- d transitions of Pr^{3+}, among these bands, the band peaked at 243 nm is considered to be the lowest $_4f^2$ – $_4f^1{}_5d^1$ transition for Pr^{3+} in the host lattice. For Fig. 4(B), the bands relating to 4f5d states were observed in the range of 220 to 340 nm, the lowest f – d transition excitation band of Ce^{3+} in $Sr_3Y(PO_4)_3$ can be observe with a peak at 304 nm (viz., 32,895 cm^{-1})) and the highest f – d transitions one of Ce^{3+} was also observed around 240 nm (viz., 41, 667 cm^{-1}).

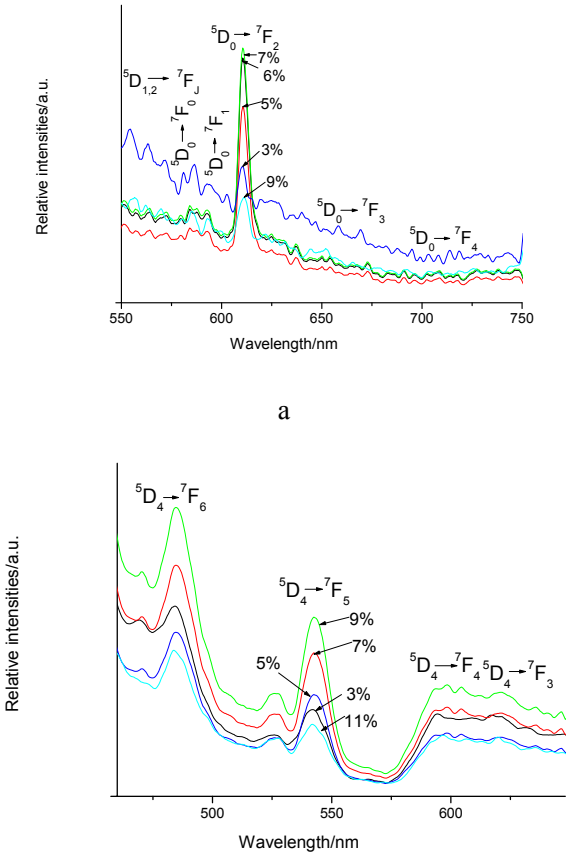

Fig. 5 Emission spectra of $Sr_3Y(PO_4)_3$: Eu^{3+} (A) and $Sr_3Y(PO_4)_3$: Tb^{3+} (B) with different doping concentration.

As shown in Fig. 5 (A), the representative emission spectrum of $Sr_3Y(PO_4)_3$: 0.05 Eu^{3+} is composed of $^5D_0 \rightarrow {}^7F_J$ (J = 0, 1, 2, 3) emission lines of Eu^{3+}, with the hypersensitive red emission transition $^5D_0 \rightarrow {}^7F_2$ being the most prominent group, which peaks at 618 nm. When the Eu^{3+} is located at low symmetry local site (without inversion center), the hypersensitive transition $^5D_0 \rightarrow {}^7F_2$ is often dominated in its emission spectrum. According to group theory selection rules, the magnetic dipole and the electric dipole are permitted and the electric dipole transition is stronger. Moreover, we can also find that the luminescent properties strongly depend on the doping concentration in $Sr_3Y(PO_4)_3$. When the concentration of Eu^{3+} increases up to 7 mol %, the intensity shows the strongest and slowly decreases at higher doping

concentrations. This is a typical property named concentration quenching of lanthanide-doped system due to mutual Eu^{3+} – Eu^{3+} interactions. Upon UV excitation, we also obtain the emission spectra of $Sr_3Y(PO_4)_3$: Tb^{3+}, which contains exclusively the characteristic transition lines of Tb^{3+} (Fig. 5 (B)). The emission peaks are centered at 490 nm ($^5D_4 \rightarrow {}^7F_6$), 543 nm ($^5D_4 \rightarrow {}^7F_5$), 590 nm ($^5D_4 \rightarrow {}^7F_4$) and 620 nm ($^5D_4 \rightarrow {}^7F_3$), respectively. The concentration quenching also appears as for the system of Tb – doped phosphors and we obtain $Sr_3Y(PO_4)_3$: Tb^{3+} the optimum dopant concentrations, which is 9 mol %. As for $Sr_3Y(PO_4)_3$: Pr^{3+} (Fig. 6), two apparent luminescent band have been observed, corresponding to the blue emission lines at 489 nm ($^3P_0 \rightarrow {}^3H_4$) and the red emission lines at 628 nm ($^3P_0 \rightarrow {}^3H_6$).

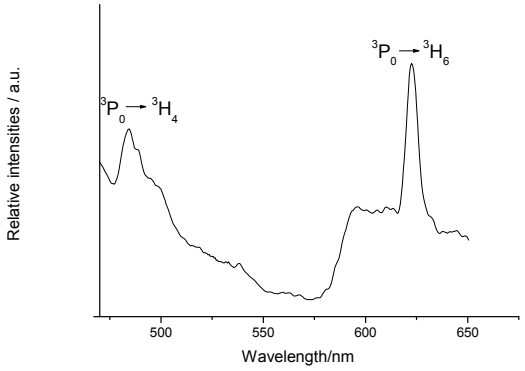

Fig. 6 Emission spectra of $Sr_3Y(PO_4)_3$: Pr^{3+}

It was well known that the trivalent Ce^{3+} - ions have an electronic structure containing one 4f – electron and as an activator, the generally result in phosphors having broad bands UV emission. The stokes shift of the Ce^{3+} emission is never very large and varies from a thousand to a few thousand wave numbers and the spectral position of the emission band depends on three factors, covalency, crystal field splitting of the $5d^1$ configuration and the stokes shift [10]. Fig. 7 (A) shows the emission spectrum of $Sr_3Y(PO_4)_3$: 0.03 mol % Ce^{3+}. It can be observed that there exists a strong broad band centered at 380 nm with a shoulder band at the short – wavelength side, corresponding to $^5D_2 - {}^7F_{7/2}$ and $^5D_2 - {}^7F_{5/2}$ transitions of Ce^{3+}. Furthermore, in order to investigate the crystal field depression value D (Ln, A) of $Sr_3Y(PO_4)_3$ the following expression was introduced:

$$D(Ln, A) = E(Ln, free) - E(Ln, A) \quad [29]$$

which is defined as the lowering of this energy when the Ce3+ ion is doped in compound; here the parameter A represents the compound name. It was reported that the energy E (Ln, free) of the first fd transition of Ce3+ as a free (gaseous) ion is 49, 340 cm^{-1} [30] and the f – d excitation transition of Ce^{3+}, E (Ce, A) we found was at 304 nm (viz., 32,895 cm^{-1}). So we can calculate that the f –d transition energy of Ce3+ in $Sr_3Y(PO_4)_3$ is depressed by 16, 895 cm^{-1} [31]. Furthermore, we can observe that the fluorescence intensity increase with an increase in Ce concentration up to 3 mol %, beyond which, the fluorescence intensity tends to quench (Fig. 7 (B)). It is also noticed that the peak positions of the emission bands have also changed significantly. However, these phosphors are emitting in the UV region, we could not compute the color coordinates.

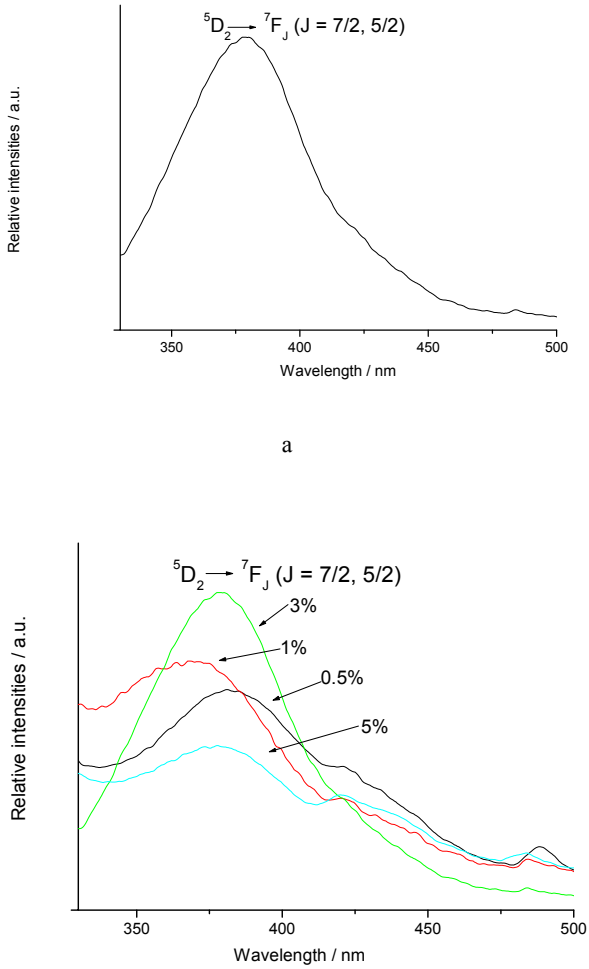

Fig. 7 Emission spectra of $Sr_3Y(PO_4)_3$: 0.03 mol % Ce^{3+} (A) and $Sr_3Y(PO_4)_3$: Ce^{3+} (B) with different doping concentration.

4. Conclusions

In summary, ternary orthophosphates $Sr_3Y(PO_4)_3$: Eu^{3+}, Tb^{3+}, Ce^{3+}, Pr^{3+} phosphors with different doping concentration were achieved by a novel in-situ assembling hybrid precursor co-precipitation technology. The characteristic emission lines of rare earth ions have been

detected and the optimum concentration of Eu^{3+} were found to be 7 mol %, for Tb^{3+} is 9 mol % and for Ce^{3+} is 3 mol %. Furthermore, we also have calculated the crystal field depression of $Sr_3Y(PO_4)_3$ host by the lowest excitation energy of Ce^{3+} when the host was doped with Ce^{3+}, which is 16, 895 cm^{-1}.

Acknowledgements

The work was supported by the Science Fund of Shanghai University for Excellent Youth Scientists and National Natural Science Foundation of China (20301013).

References

[1] D. J. Segal, R.P. Santoro, R.E. Newnham, Zeit. Kristallog. **123,** 1 (1966).
[2] G. Blasse, J Solid State Chem. **2**, 27 (1970).
[3] G. Engel, W. Kirchberger, Z Anorg Allg Chem. **417**, 81 (1975).
[4] G. J. MacCarthy, D. E Pfoertsch, J Solid State Chem. **38**, 128 (1981).
[5] P. Fischer, F. Waldner, Solid State Commun. **44**, 657 (1982).
[6] T. Tsuboi, H.J. Seo, B. K. Moon, J.H. Kim, Physica B **45**, 270 (1999).
[7] E.H. Arbib, B. Elouadi, J.P. Chaminade, J. Darriet, Mater. Res. Bull. **35**, 761 (2000).
[8] D. M. Burland, R.D. Miller and C. A. Walsh, Chem. Rev., **94**, 31 (1994).
[9] L. L. Beecroft and C. K. Ober, Chem. Mater., **9**, 1302 (1997).
[10] G. Blasse, B. C. Grabmeter, Luminescent Materials, Springer Verlag; Berlin, (1994).
[11] L. Hesselink, S.S. Orlov, A. Liu, A. Akella, D. Lande, R. R. Neurgaonkar, Science, **282**, 1089 (1998).
[12] W. Rehwald, R. Widmer, J Phys Chem Solids **34**, 2269 (1973).
[13] F. Rogemond, C. Pedrini, B. Moine, G. Boulon, J Lumin. **33**, 455 (1985).
[14] A. A Kaminskii, O. Schultze, B. Hermoneit, S. E. Sarkisov, L. L. J. Bohm, P. Reichter, R. Ehlert, A. A. Mayer, Y. A. Lomonov, V. A. Balashov, Phys Status Solidi A **33**, 737 (1976).
[15] A. Chagraoui, DES de 3e`me Cycle de Spe´cialite´, Faculty of Sciences, Rabat, Morocco, 1987.
[16] F. De Notaristefani, P. Lecoq, M. Schneegans, Heavy Scintillators, Editions Frontie`res, Gif-sur-Yvette, Paris, 1993.
[17] M. F. Hoogendop, W.J. Schipper, G. Blasse, J Alloy. Compd. **205**, 249 (1994).
[18] H. B Liang, Y. Tao, J. H. Xu, H. He, H. Wu, W. X. Chen, S. B Wang, Q. Su, J. Solid State Chem. **177**, 901 (2004).
[19] Y. Yu, S. H. Zhou, S. Y. Zhang, J. Alloy. Compd. **351**, 84 (2003).
[20] E. Cavalli, M. Bettinelli, A. Belletti, A. Speghini, J. Alloy. Compd. **341**, 107 (2002).
[21] B. Yan, L. Zhou, J. Alloy. Compds. **372**, 238 (2004).
[22] B. Yan, H. H. Huang, J. Mater. Sci. Lett. **39**, 3529 (2004).
[23] B. Yan, X. Z Xiao, Opt. mater. **28**, 498 (2006).
[24] X. Z. Xiao, B. Yan, J. Non – Cryst. Solids **351**, 3634 (2005).
[25] H. H. Huang, B. Yan, Solid state commun. **132**, 773 (2004).
[26] X. Q. Su, B.Yan, H. H. Huang, J. Alloys Compds. **399**, 227 (2005).
[27] J. F. Ma, Z. S. Jin, J. Z. Ni, Chin. J. Inorg. Chem. **9**, 160 (1993).
[28] X. H. Chuai, H. J. Zhang, F. S. Li, Mater. Lett. **46**, 244 (2000).
[29] 1. M. V. Hoffman, J. Electrochem. Soc: Solid State Sci. **115**, 560 (1968).
[30] P. Dorenbos, J. Lumin. **91**, 155 (2000).
[31]H. B. Liang, Y. Tao, Q. Su, S.B. Wang, J. Solid State Chem. **167**, 435 (2002).

*Corresponding author: byan@tongji.edu.cn